BIOCHEMISTRY
including biophysical chemistry & molecular biology

Article

pubs.acs.org/biochemistry

Heme Binding Constricts the Conformational Dynamics of the Cytochrome b_{559}' Heme Binding Cavity

Yasar Akdogan,[‡] Veerappan Anbazhagan,[†] Dariush Hinderberger,*[,‡] and Dirk Schneider*[,†]

[†]Institut für Pharmazie und Biochemie, Johannes Gutenberg-Universität Mainz, Johann-Joachim-Becher-Weg 30, 55128 Mainz, Germany

[‡]Max Planck Institute for Polymer Research, Ackermannweg 10, 55128 Mainz, Germany

Supporting Information

ABSTRACT: Cytochrome b_{559}' is a transmembrane protein formed by homodimerization of the 44-residue PsbF polypeptide and noncovalent binding of a heme cofactor. The PsbF polypeptide can dimerize in the absence and presence of heme. To monitor structural alterations associated with binding of heme to the apo-cytochrome, we analyzed the apo- and holo-cytochrome structure by electron paramagnetic resonance spectroscopy. Spin labeling of amino acids located close to the heme binding domain of the cytochrome revealed that the structure of the heme binding domain is unconstrained in the absence of heme. Heme binding restricts the conformational dynamics of the heme binding domain, resulting in the structurally more constricted holo-cytochrome structure.

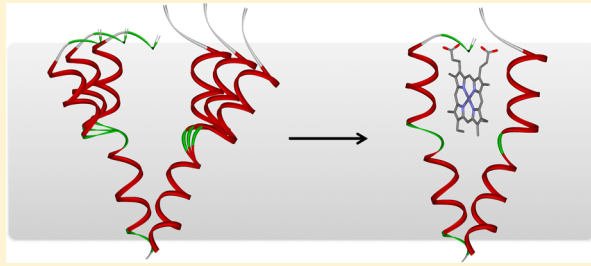

Interactions of individual transmembrane (TM) helices and the specific role of individual amino acids or of amino acid motifs in the formation of higher-order TM helix bundles have been analyzed in some detail in recent years. However, while many membrane proteins contain essential cofactors, which are tightly bound in the membrane plane region, contributions of cofactor binding to folding and stability of TM proteins have been analyzed far less. The two TM proteins cytochrome b_6 and cytochrome b_{559}' have turned out in recent years to be excellent models for studying the impact of noncovalent heme binding to TM apo-cytochromes.[1−7] The cytochrome b_{559}' model is a homodimer of the 44-residue PsbF polypeptide, which spans the membrane with a single TM helix.[7,8] In vivo, the two peptides, PsbE and PsbF, each span the membrane once and together form the heterodimeric cytochrome b_{559},[9] a photosystem II subunit, which can act as an electron donor to photosystem II when electron transfer resulting from water oxidation is inhibited.[10] While PsbE and PsbF differ in their extramembrane regions, amino acids responsible for dimerization and cofactor binding are conserved within the TM domains of the two polypeptides.[7] Thus, the heme binding PsbF homodimer (cytochrome b_{559}') can serve as a minimal TM cytochrome model. The TM helix dimerization domain (Ser29−Met39) of PsbF is separated from the heme binding domain (Val17−Val27) by a conserved Pro kink, which is essential for formation of the holo-cytochrome structure.[7,11] Dimerization of PsbF TM helices does not require binding of the heme cofactor.[12] In contrast, TM helix−helix interaction and apo-cytochrome formation are prerequisites for heme binding and assembly of the holo-cytochrome.[7,13] However, while dimerization of the PsbF peptide does not depend on heme binding, the structure of the apo-cytochrome might differ from the structure of the holo-cytochrome. As heme binding or mutations of amino acids located in the cytochrome b_{559}' heme binding domain do not affect the dimerization propensity of the TM helix,[7] the structure of the dimerization domain does probably not differ significantly. However, it is not clear if the heme binding domain is more flexible in the absence of heme or if a rigid, preformed heme binding cavity is a prerequisite for incorporation and binding of the heme cofactor. In the case of the soluble cytochrome b_{562}, it has, for example, been observed that the secondary structure of the heme-free apo-cytochrome appeared to be largely preserved whereas the global folding was only partially completed.[14,15] While heme binding TM four-helix bundle proteins, such as the first four TM helices of cytochrome b, have extensively been used as templates for the design of TM b-type cytochromes, only very recently has a simpler TM b-type cytochrome been designed.[16,17] Here, the stable and rigid glycophorin A (GpA) TM helix dimer has been used as a scaffold, and after the insertion of heme-ligating residues, the GpA homodimer binds heme, though only with a low affinity. Analyzing the folding, assembly, and stability of a simple TM b-type cytochrome model, which was "designed" by nature, might allow the deduction of principles guiding the improved design of simple TM cytochromes. In particular, revealing the dynamics and remodeling of local structures involved in heme binding might help to improve simple TM cytochrome models, as the low heme binding affinity of the GpA model might be caused by the overly structurally inflexible apoprotein structure predefined by the GpA scaffold.

Received: April 16, 2012
Revised: August 13, 2012
Published: August 16, 2012

Electron paramagnetic resonance (EPR) spectroscopy in combination with site-directed spin labeling (SDSL) is a powerful method for studying the structure and conformational dynamics of soluble proteins[18−20] and has already been successfully applied to study the structure, folding, or structural dynamics involved in the activity of α-helical TM proteins.[21−25] In SDSL-EPR, a nitroxide label is attached to an introduced cysteine in a protein. Furthermore, protein labeling at two different cysteines can be used to assess the local structure of proteins by measuring magnetic dipolar coupling (through space) between the two attached radicals and extracting distances up to 2 nm by continuous wave (CW) EPR spectroscopy and distances up to 8 nm by double electron−electron resonance (DEER) spectroscopy.[26−28] If the two spin centers of the radicals approach each other closely or even collide, their spin states may change because of the collision and subsequent overlap of spin-bearing orbitals, an effect called spin exchange. The impact of spin exchange on CW EPR spectra can be used to obtain quantitative information about collision rates of molecules, activation energies of spin exchange, and steric hindrance in collisions.[29] In particular, the conformational flexibility of macromolecules (polymers, proteins, etc.) can be studied using spin exchange that occurs when their electron-carrying orbitals overlap.[30]

To assess the structural dynamics associated with cofactor binding, we have analyzed the local flexibility of the cytochrome b_{559}' heme binding domain in the absence and presence of heme by EPR spectroscopy using spin-labeled PsbF peptides. On the basis of the results, the apo-cytochrome structure appears to involve a flexible heme binding domain and heme binding constricts this local flexibility.

MATERIALS AND METHODS

The PsbF peptide (MATQNPNQPVTYPIFTVRWCAVHTLAVPSVFFVGAIAAMQFIQR) was custom synthesized. At position 20, the naturally occurring Leu residue was replaced with a Cys (underlined). A 3-maleimido-PROXYL (3-maleimido-2,2,5,5-tetramethyl-1-pyrrolidinyloxyl) spin-label was coupled to the cysteine residue, and the labeled peptide was purified by high-performance liquid chromatography. The purity of the peptide was analyzed by mass spectrometry (Peptide Specialty Laboratories GmbH, Heidelberg, Germany).

Detergent Reconstitution of Holo-Cytochrome b_{559}'. Lyophilized peptides were dissolved in 2,2,2-trifluoroethanol. Solvents were subsequently removed under a gentle stream of nitrogen gas, and final traces of the solvents were removed by vacuum desiccation for 3 h. The dried peptide films were reconstituted in 10 mM phosphate buffer (pH 7.4), 150 mM NaCl, and 10 mM SDS. For reconstitution, the PsbF peptide was mixed with heme in a 2:1 ratio, as cytochrome b_{559}' is a PsbF homodimer, which binds one heme molecule. Incorporation of heme and cytochrome assembly was monitored by absorbance spectroscopy using a Perkin-Elmer Lambda 35 UV−vis spectrophotometer. Spectra were recorded from 350 to 600 nm with a resolution of 0.5 nm. The heme concentration was determined spectroscopically using an extinction coefficient (ε_{385}) of 56 mM^{-1} cm^{-1}.

Circular Dichroism Spectroscopy. Circular dichroism (CD) spectra were recorded at 25 °C on a Jasco J-810 spectropolarimeter at a scan speed of 20 nm/min using a 0.1 cm path-length quartz cuvette. Far-UV CD spectra were recorded at a peptide concentration of 10 μM. Data were collected with a response time of 2 s and a slit width of 1 nm. Each reported spectrum is the average of three consecutive scans from which buffer scans, recorded under the same conditions, were subtracted. For comparison between different samples and to verify the average secondary structure content, the measured ellipticity was converted to mean residue ellipticity by

$$\text{mean residue ellipticity} = 100\theta/(cnl) \quad (1)$$

where θ is the measured ellipticity in millidegrees, c the peptide concentration in micromolar, n the number of amino acids in the peptide, and l the path length in centimeters. Peptide concentrations were determined from absorbance measurements using a Perkin-Elmer Lambda 35 UV−vis spectrophotometer.

EPR Spectroscopy. A Miniscope MS200 (Magnettech, Berlin, Germany) benchtop spectrometer was used for CW EPR measurements at a microwave frequency of ∼9.4 GHz (X-band). Measurements were performed at different temperatures between 303 and 323 K using a modulation amplitude of 0.05 mT. The microwave frequency was recorded with a model 2101 frequency counter (Racal-Dana).

Low-temperature X-band EPR experiments at 50 K were performed with a Bruker Elexsys 580 spectrometer equipped with a Bruker Flexline split-ring resonator ER4118X_MS3.[31,32] The field-swept, electron spin echo-detected EPR spectra were recorded by integrating the intensity of the two-pulse echo (π/2−τ−π−echo) observed as a function of the field position. The pulse lengths were 16 ns (π/2) and 32 ns (π) with an interpulse delay of 184 ns (τ).

Both, EPR measurements at high and low temperatures were performed with 0.42 mM spin-labeled peptide after the addition of 20% glycerol by volume.

Data Analyses. The EPR spectra were background-corrected using a home-written Matlab program. The pseudomodulated ESE spectrum was obtained with a home-written Matlab program employing Easyspin version 3.0.0. Simulations were also performed with Matlab-based Easyspin version 3.0.0.[33] The EPR parameters obtained for the holo-cytochrome were as follows: g_{xx} = 2.0084, g_{yy} = 2.0051, g_{zz} = 2.0022, A_{xx} = A_{yy} = 16.8 MHz, and A_{zz} = 99.4 MHz at 303 K, and g_{xx} = 2.0088, g_{yy} = 2.0055, g_{zz} = 2.0025, A_{xx} = A_{yy} = 19.8 MHz, and A_{zz} = 102 MHz at 50 K. For apo-cytochrome, they were as follows: g_{xx} = 2.0088, g_{yy} = 2.0055, g_{zz} = 2.0025, A_{xx} = A_{yy} = 19.8 MHz, and A_{zz} = 103 MHz at 50 K. The EPR parameters of the 3-maleimido-PROXYL label at 223 K (g_{xx} = 2.0084, g_{yy} = 2.0061, g_{zz} = 2.0025, A_{xx} = A_{yy} = 17.7 MHz, and A_{zz} = 101.0 MHz) were taken from data obtained analyzing spin-labeled human serum albumin.[34]

DEER Spectroscopy. The four-pulse DEER sequence π/2(ν_{obs})−τ_1−π(ν_{obs})−(τ_1+t)(ν_{pump})−(τ_2−t)−π(ν_{obs})−τ_2−echo was used to obtain dipolar time evolution data at X-band frequencies (∼9.4 GHz). DEER experiments were performed on a Bruker Elexsys 580 spectrometer equipped with a Bruker Flexline split-ring resonator ER4118X_MS3.[31,32] The dipolar evolution time t was varied; τ_2 was 2.5 μs, and τ_1 was kept constant. Proton modulation was averaged by the addition of eight time traces of variable τ_1 values, starting with a $\tau_{1,0}$ of 200 ns and incrementing by a $\Delta\tau_1$ of 8 ns.[35] The resonator was overcoupled to $Q \approx 100$. The pump frequency, ν_{pump}, was set to the maximum of the echo-detected (absorption) EPR spectrum. The observer frequency, ν_{obs}, was set to ν_{pump} + 61.6 MHz, coinciding with the low-field local maximum of the nitroxide spectrum. The observer pulse lengths were 32 ns for

dx.doi.org/10.1021/bi300489s | Biochemistry 2012, 51, 7149−7156

both $\pi/2$ and π pulses, and the pump pulse length was 12 ns. The temperature was set to 50 K by cooling with a closed cycle cryostat (ARS AF204, customized for pulse EPR, ARS, Macungie, PA). The raw time domain DEER data were processed with DeerAnalysis2008.[35,36] DEER measurements were performed with 0.42 mM spin-labeled peptide after addition of 20% glycerol by volume.

RESULTS AND DISCUSSION

Characterization of Spin-Labeled Peptides. On the basis of the available PsbF structure,[37] we introduced a spin-label at position 20 of the PsbF peptide. Therefore, during synthesis the original Leu was replaced with a Cys residue. As in the original cytochrome b_{559} structure, this amino acid side chain is not in contact with residues from the adjacent helix, subsequent attachment of the PROXYL spin-label at the cysteine side chain can be assumed not to interfere with PsbF helix formation and cytochrome assembly. While at this position the C_α atoms of the amino acids on the two PsbF peptides of each monomer of the homodimer are at a distance of approximately 1.8 nm, the length and mobility of the spin-labeled side chains allow increased or decreased distances between the actual spin-probes. Thus, the spin-probes might be at a distance region that is borderline in sensitivity between CW EPR and DEER (~1.5 nm).

To exclude the possibility that the introduced spin-label affects secondary structure formation of the PsbF peptide, we recorded far-UV CD spectra of the PsbF peptide (Figure 1). The CD spectra show double minima near 208 and 222 nm, which are characteristic of an α-helical structure. The spectra of the labeled and unlabeled peptides are essentially identical, indicating that spin labeling of the amino acid does not affect secondary structure formation of the PsbF peptide. Furthermore, also after addition of heme and in vitro reconstitution of holo-cytochrome b_{559}', the far-UV CD spectra are virtually identical, regardless of whether unlabeled or spin-labeled peptides were used. These results indicate that the secondary structure of the labeled PsbF peptide is well preserved under the experimental conditions.

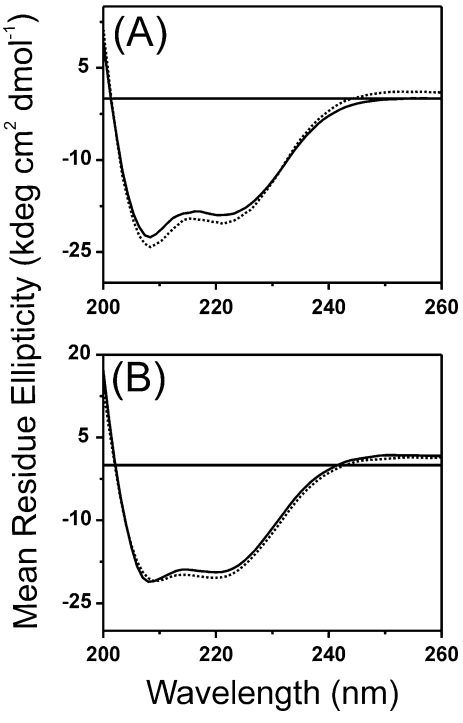

Figure 1. Secondary structure of the PsbF peptide. (A) Far-UV CD spectra of unlabeled (—) and spin-labeled PsbF (···) peptides measured in 10 mM SDS. (B) Far-UV CD spectra of the spin-labeled PsbF peptide measured in the absence (—) and presence (···) of heme at a peptide:heme ratio of 2:1. CD spectra were measured at a peptide concentration of 20 μM in 10 mM SDS. The measured ellipticity was converted to mean residue ellipticity as described in Materials and Methods.

Heme binding and assembly of holo-cytochrome b_{559}' were tested by absorption spectroscopy (Figure 2). To monitor holo-cytochrome formation, detergent-solubilized peptides were mixed with heme at a peptide:heme ratio of 2:1. Addition of heme to the spin-labeled PsbF peptide shifted the Soret band maximum from 404 nm, which corresponds to free heme, to 413 nm, which indicates successful in vitro reconstitution and assembly of holo-cytochrome b_{559}'. Together, absorbance and CD spectroscopy suggest that the introduced spin-label neither affects the PsbF secondary structure nor significantly interferes with holo-cytochrome formation.

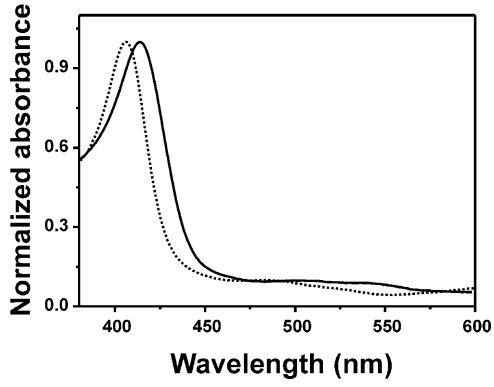

Figure 2. In vitro assembly of cytochrome b_{559}' using spin-labeled PsbF peptides. Absorbance spectra of free heme (—) and cytochrome b_{559}' (···) assembled from spin-labeled peptides. Spectra were recorded in 10 mM SDS at a peptide:heme ratio of 2:1 and are normalized at the absorbance maximum at ~400−420 nm.

CW EPR Spectra of Apo- and Holo-Cytochrome b_{559}'. CW EPR spectra of the spin-labeled PsbF homodimer in the presence and absence of heme were measured at 303 K. After the addition of heme, the EPR spectrum of the cytochrome mainly displayed the usual three-line pattern because of hyperfine interaction of each unpaired electron with the nuclear magnetic moment of one ^{14}N nucleus with nuclear spin $I_N = 1$[18] (Figure 3A). Besides the three-line pattern, a weak, broad underlying single line was observed. Figure 3A shows the measured CW EPR spectrum of the holo-cytochrome together with simulations obtained by addition of the simulated three-line pattern and a broad signal that contributes 11% to the overall spectral intensity (as gained from the spectral simulations).

The EPR spectrum of the spin-labeled PsbF peptides in the absence of heme (Figure 3B) reveals two features that cannot be explained by considering solely a spin-labeled monomer: there is a much stronger contribution of the strong broad signal underlying the usual three-line spectrum (compare Figure 3A), and weak signals between the three sharp signals appear in addition. The broad signal might stem from peptide aggregates or precipitates. Strong interactions of spin-labels with each

dx.doi.org/10.1021/bi300489s | Biochemistry 2012, 51, 7149−7156

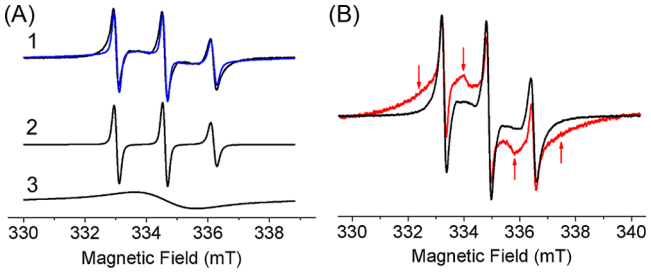

Figure 3. (A) CW EPR spectra at X-band of spin-labeled PsbF in the presence of heme (black) at 303 K and its simulation (blue) (1). The simulation of the spectrum was obtained by addition of simulated three-line spectra (g_{xx} = 2.0084, g_{yy} = 2.0051, g_{zz} = 2.0022, A_{xx} = A_{yy} = 16.8 MHz, and A_{zz} = 99.4 MHz) (2) and a simulated broad signal (3) with an intensity ratio of 9:1. (B) Comparison of CW EPR spectra of spin-labeled PsbF in the absence (red) and presence (black) of heme measured at 303 K. The differences between the two cases are denoted with red arrows. The two arrows in the center indicate the biradical signatures.

other in larger aggregates can lead to the collapse of the three hyperfine lines into a broad single line. Because at this peptide concentration (0.42 mM) the broad component is far less pronounced in the case of the holo-cytochrome (Figure 3A), heme binding appears to efficiently stabilize the peptide structure against aggregation, which indicates structural alterations or altered self-assembly. The second difference in the EPR signatures is that without heme the spin-labeled PsbF dimer displays two weak additional signals, which are typical for a CW EPR spectrum of biradicals exhibiting spin exchange interaction.[29,30,38] Spin exchange as an interspin interaction is a direct consequence of collisions of a defined lifetime between the radicals, during which the spin (electron)-bearing molecular orbitals physically overlap. The strength of spin exchange can be quantified by the exchange integral J. In a biradical system, in the absence of spin exchange (exchange integral $J = 0$), the two spin-labels behave as two independent radicals and yield three lines (^{14}N nuclear spin $I_N = 1$) separated by a, the nitrogen hyperfine splitting. If there is a strong spin exchange interaction ($J \gg a$) between the two spin-labels, the spectrum consists of five lines separated by $a/2$.[39] In a situation where the value of the exchange integral is between the two values ($J > a$), the widths of the three original single radical lines are unaffected but the two additional lines are broadened, and this broadening is determined by the value of the exchange integral.[40] Although the spectra of the system without heme (Figure 3B) correspond to the $J > a$ case, the analysis of experimental results, especially for polymers or proteins, requires consideration of different conformations with nonequivalent J values. The dynamic behavior of such macromolecules at ambient temperatures can simply be explained by the superposition of the EPR spectral features stemming from different conformations.[29,30] On the basis of our observations, it appears reasonable to qualitatively argue that the spin-label binding sites are flexible in the PsbF dimer when heme is absent, which allows interaction (collision) of spin-labels. However, the presence of heme between the PsbF monomers appears to induce a barrier and prevents spin exchange. Thus, either the interaction of spin-labels is sterically directly hindered by the bound heme, or the flexibility of the peptide is restricted in an indirect manner. Importantly, in both cases, the dynamics and/or steric constraints of the monomers are such that they cannot approach each other close enough for significant intermolecular spin exchange.

Generally, the temperature dependence of the spin exchange rate in long chain biradicals (polymers) can be described by the Arrhenius equation. The activation energy of spin exchange is obtained from the Arrhenius plot of the intensities or the line widths of the spin exchange (I_b) and the monoradical (I_m) components of the EPR spectrum versus inverse temperature.[29,30,38,41] A low activation energy for spin exchange is related to more direct, less hindered collisions of the monoradical fragments. Furthermore, when line narrowing and increasing intensities of the "biradical" component (spectral component I_b) can be observed with an increasing temperature, this is indicative of faster spin exchange.[38,42] Figure 4A shows CW EPR spectra of the spin-labeled PsbF peptides at different temperatures. As expected for spin exchanging species, the relative intensity of the spin exchange components (biradical, I_b) increases with temperature in the spectra normalized to the intensity of the central peak (noninteracting monoradicals, I_m). However, the effect of temperature is still not adequate to calculate the activation energy of spin exchange from the line narrowing (of the non-spin exchanging component), as the structure of the peptide might be temperature-dependent. Nonetheless, an effect of temperature on the spin exchange mechanism is clearly detectable from the intensity ratio of the species with spin exchange to the species without spin exchange (I_b/I_m). The activation energy of spin exchange interactions (E_a = 10 kcal/mol) can then be estimated from the Arrhenius dependence of the I_b/I_m ratio and the temperature (Figure 4B). On the other

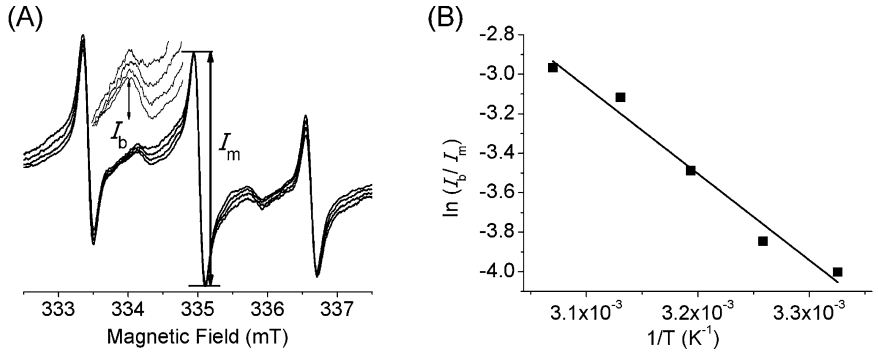

Figure 4. (A) CW EPR spectra of spin-labeled PsbF in the absence of heme at 308, 313, 318, and 323 K (from top to bottom, respectively). (B) Temperature dependency of the I_b/I_m ratio for the PsbF peptide dimers from panel A. The corresponding activation energy (E_a) for spin exchange is calculated from the slope of the linearized Arrhenius-type plot.

dx.doi.org/10.1021/bi300489s | *Biochemistry* 2012, 51, 7149−7156

hand, the spectrum of the heme-containing sample only showed a trivial temperature dependence of the single radical line widths, which suggests that no spin exchange interaction ensues when heme is bound (Figure S1 of the Supporting Information).

Low-Temperature EPR Measurements. Figure 5 shows the field-swept, echo-detected (and pseudomodulated) EPR spectrum at the X-band of spin-labeled peptides in the presence and absence of heme. The line broadening of the electron spin echo-detected EPR spectrum at 50 K caused by dipolar couplings could be analyzed in terms of the distance distribution between two unpaired electron spins (spin-labels) for short distances (0.8−2 nm). As spin exchange (J coupling) at low temperature is not as effective as it is at moderate temperatures and as the J coupling is much more pronounced when the distances are shorter than approximately 0.8 nm, we obtained a rough approximation for the spin−spin distance from low-temperature experiments by just considering the dipolar coupling. The known dependence of the dipolar coupling on the interspin distance, r^{-3}, was obtained using a convolution of a relevant unbroadened EPR spectrum with the dipolar broadening function.[43] Immediate peptide dimerization at any concentration did not allow us to obtain the unbroadened monomer spectrum for reference. Therefore, the reference spectrum was approximated using the EPR parameters of the high-temperature measurements together with literature values.[34] The final EPR parameters of the simulations are given in Materials and Methods. Both, the apo- and holo-cytochrome spectra are very similar, and simulation of both was possible solely by using a large fraction of a strongly broadened spectral component (see Figure S2 of the Supporting Information). This suggests that the average distance between the heme binding helix part of the two PsbF monomers in the dimer is not affected by heme. The simulations of these spectra reveal an average and approximate distance of 1.1 nm with a fitting uncertainty of 0.1 nm (it should be noted that as stated above, this completely neglects the effect of residual exchange coupling). However, the deviation of the distances between the EPR simulations and the structural model (1.8 nm, which is the distance between the C_α atoms of the labeled amino acids) may stem from EPR spectral simulations being prone to the overemphasis of short distances, and also the distance between the actual spin centers of the spin-labels could be shorter than 1.8 nm. On the basis of these data, it appears likely that heme binding, which seems to slow or prevent side chain (spin-label) interactions between PsbF monomers, affects the side chain dynamics and local flexibility of the heme binding domain.

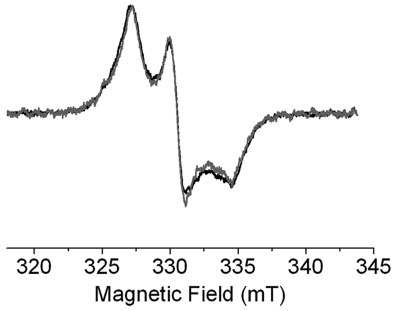

Figure 5. Echo-detected, pseudomodulated EPR spectra at X-band of 0.42 mM spin-labeled PsbF in the absence (black) and presence (gray) of heme measured at 50 K.

Nanoscale Distance Measurements Using DEER. The DEER method increases the range of distance sensitivity to 6 nm (8 nm under completely optimized conditions) by measuring dipolar couplings between unpaired electron spins. However, the lower distance limit for measuring dipolar coupling using DEER is around 1.5−1.6 nm. Therefore, the distance between spin-labels in the PsbF peptide is outside the DEER sensitivity range. However, the DEER measurements provide a negative control to show structural similarities and conformational variations in the two cases. This is important to show that heme binding does not influence the PsbF dimer structure and pushes the two spin-labels farther apart than the 1.5 nm lower bound of DEER. Importantly, the DEER measurements did not indicate any significant deviations; e.g., the time domain signals and the modulation depths are very similar, but only a small difference in the modulation properties has been observed (see the DEER part and Figure S3 of the Supporting Information).

Assembly of a Transmembrane Cytochrome Model. While most studies aiming to analyze folding of TM proteins concentrate on cofactor-less proteins, in few cases individual folding events have been analyzed using cofactor-containing TM proteins. Most extensively, plant light-harvesting complex II (LHC II) and the archaebacterial proton pump bacteriorhodopsin have been characterized, and individual folding steps have been defined. Folding of LHC II appears to be induced by binding of the cofactors, and secondary and tertiary structure formation is tightly coupled to pigment binding.[21,44−47] In contrast, bacteriorhodopsin folds into a folding intermediate in the absence of the retinal cofactor, and covalent attachment of the retinal to the apoprotein results in structural rearrangements and formation of the final, active bacteriorhodopsin structure.[48−53] Bacteriorhodopsin consists of seven TM helices, which form a complex structure and bind the retinal cofactor in the center of the helix bundle. Thus, initial folding to an intermediate structure is crucial for allowing the cofactor entering the protein core within the membrane plane, where most likely a retinal binding niche is preformed. Spontaneous covalent binding of the retinal then triggers formation of the final, stable bacteriorhodopsin structure. In the case of cytochrome b_{559}′, the situation differs significantly, as proper dimerization of the PsbF monomers does not appear to be influenced by the cofactor, and thus the structures of the apo and holo forms probably do not differ in the dimerization domain.[7,12] While it appeared possible that the heme binds to a predefined, heme binding cavity of the apo-cytochrome, the results of this study indicate that the structure of the heme binding peptide domain is more flexible in the absence of heme, at least in detergent. Thus, a rather rigid, well-defined heme binding cavity appears not to exist in the absence of heme. Heme binding and holo-cytochrome formation restrict the conformational flexibility of the (spin-labeled) heme binding domain, at least for parts of the ensemble. As the analyzed peptides are strongly hydrophobic, only SDS could be used to properly analyze interactions of the peptides. Luckily, SDS is well-known to allow proper packing of many TM helices,[54] and the results shown in Figures 1 and 2 demonstrate that the PsbF secondary structure is not affected by SDS and the cytochrome assembles. However, it appears to be likely that the cytochrome structure is weakened in SDS micelles. Thus, flexibility might be reduced in milder detergents or in a membrane environment.

dx.doi.org/10.1021/bi300489s | *Biochemistry* 2012, 51, 7149−7156

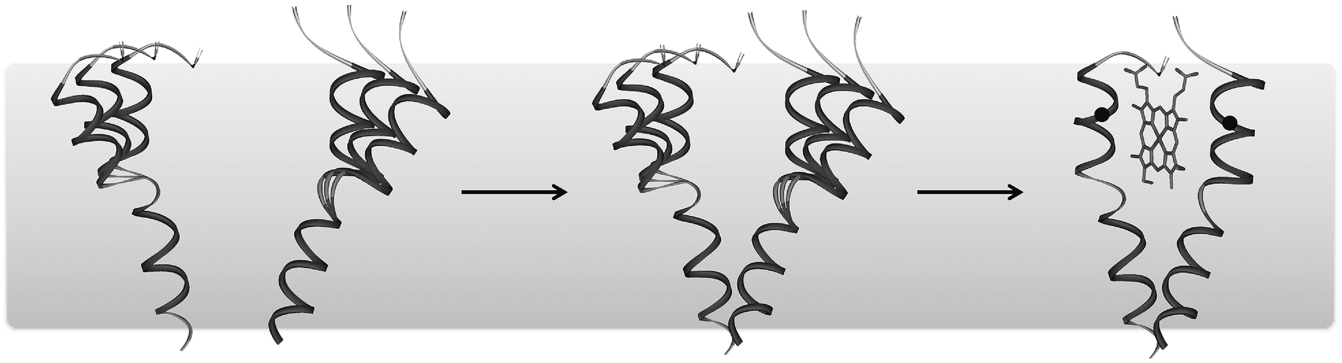

Figure 6. Multistep assembly of cytochrome b_{559}'. The monomeric PsbF TM peptides interact and form a homodimer with a flexible heme binding domain. Heme binding constricts the flexibility, resulting in formation of the final cytochrome structure. The position of the spin-labels is indicated in the holo-cytochrome structure by black marks.

Together, our results indicate that assembly of cytochrome b_{559}' involves multiple steps (Figure 6): individual PsbF helices display some flexibility in their heme binding domain, and thus, the structure of the peptide is flexible. Dimerization results in interaction of the PsbF dimerization domain, in tight packing, and in stable dimer formation. However, dimerization does not restrict the conformational flexibility of the heme binding domain, and a flexible heme binding cavity is predefined. Only after binding of the heme cofactor does the final holoprotein structure emerge and a stable, structurally well-defined holo-cytochrome form. This finding might explain why insertion of a simple heme binding amino acid motif into the TM helix of the human GpA TM helix resulted in the formation of a TM helix dimer with low heme binding affinity.[16] Structural dynamics and a flexible heme binding cavity might be crucial for efficient heme entry and binding to minimal heme binding TM helix dimers. Formation of a structurally not entirely defined and flexible rather than of a well-defined, rigid heme binding cavity might be crucial for the design of simple TM cytochrome models with increased heme binding affinities. Allowing structural flexibility, as here observed with cytochrome b_{559}', in designed porphyrin-binding TM proteins might allow an improved de novo design of porphyrin-binding, electron-transferring TM proteins.

■ ASSOCIATED CONTENT

Supporting Information

CW EPR spectra of spin-labeled PsbF in the presence of heme at different temperatures (Figure S1), echo-detected, pseudo-modulated EPR spectra at X-band of spin-labeled PsbF in the absence and presence of heme at 50 K together with their simulations (Figure S2), and DEER measurements of spin-labeled PsbF in the absence and presence of heme (Figure S3). This material is available free of charge via the Internet at http://pubs.acs.org.

■ AUTHOR INFORMATION

Corresponding Author

*D.S.: phone, +49 6131 39-25833; e-mail, dirk.schneider@uni-mainz.de. D.H.: phone, +49 6131 379-126; e-mail, dariush.hinderberger@mpip-mainz.mpg.de.

Author Contributions

Y.A. and V.A. contributed equally to this work.

Funding

This work has been supported by grants from the Deutsche Forschungsgemeinschaft (SCHN 690/2-3), the German-Israeli foundation, the center of complex matter (COMATT), the University of Mainz, the Max Planck Society, and the Max Planck Graduate Center with the University of Mainz (MPGC). Y.A. thanks the Max Planck Society for a stipend.

Notes

The authors declare no competing financial interest.

■ ACKNOWLEDGMENTS

We thank J. Klare for helpful suggestions during the initial stage of this project and H. Pearson and J. Neumann for carefully proofreading the manuscript.

■ REFERENCES

(1) Weber, M., Prodohl, A., Dreher, C., Becker, C., Underhaug, J., Svane, A. S., Malmendal, A., Nielsen, N. C., Otzen, D., and Schneider, D. (2011) SDS-facilitated in vitro formation of a transmembrane b-type cytochrome is mediated by changes in local pH. *J. Mol. Biol. 407*, 594−606.

(2) Dreher, C., Prodöhl, A., Hielscher, R., Hellwig, P., and Schneider, D. (2008) Multiple step assembly of the transmembrane cytochrome b6. *J. Mol. Biol. 382*, 1057−1065.

(3) Prodöhl, A., Weber, M., Dreher, C., and Schneider, D. (2007) A mutational study of transmembrane helix-helix interactions. *Biochimie 89*, 1433−1437.

(4) Prodöhl, A., Dreher, C., Hielscher, R., Hellwig, P., and Schneider, D. (2007) Heterologous expression and in vitro assembly of the transmembrane cytochrome b6. *Protein Expression Purif. 56*, 279−285.

(5) Koch, H. G., and Schneider, D. (2007) Assembly and stability of transmembrane cytochromes. *Curr. Chem. Biol. 1*, 59−74.

(6) Dreher, C., Prodöhl, A., Weber, M., and Schneider, D. (2007) Heme binding properties of heterologously expressed spinach cytochrome b_6: Implications for transmembrane b-type cytochrome formation. *FEBS Lett. 581*, 2647−2651.

(7) Prodöhl, A., Volkmer, T., Finger, C., and Schneider, D. (2005) Defining the structural basis for assembly of a transmembrane cytochrome. *J. Mol. Biol. 350*, 744−756.

(8) Francke, C., Loyal, R., Ohad, I., and Haehnel, W. (1999) In vitro assembly of a β2 cytochrome b559-like complex from the chemically synthesised β-subunit encoded by the *Synechocystis* sp. 6803 psbF gene. *FEBS Lett. 442*, 75−78.

(9) Stewart, D. H., and Brudvig, G. W. (1998) Cytochrome b559 of photosystem II. *Biochim. Biophys. Acta 1367*, 63−87.

(10) Shinopoulos, K. E., and Brudvig, G. W. (2012) Cytochrome b559 and cyclic electron transfer within photosystem II. *Biochim. Biophys. Acta 1817*, 66−75.

(11) Weber, M., Tome, L., Otzen, D., and Schneider, D. (2012) A Ser residue influences the structure and stability of a Pro-kinked transmembrane helix dimer. *Biochim. Biophys. Acta 1818*, 2103−2107.

(12) Volkmer, T., Becker, C., Prodöhl, A., Finger, C., and Schneider, D. (2006) Assembly of a transmembrane b-type cytochrome is mainly driven by transmembrane helix interactions. *Biochim. Biophys. Acta 1758*, 1815−1822.
(13) Volkmer, T., Becker, C., Prodohl, A., Finger, C., and Schneider, D. (2006) Assembly of a transmembrane b-type cytochrome is mainly driven by transmembrane helix interactions. *Biochim. Biophys. Acta 1758*, 1815−1822.
(14) Fuentes, E. J., and Wand, A. J. (1998) Local stability and dynamics of apocytochrome b562 examined by the dependence of hydrogen exchange on hydrostatic pressure. *Biochemistry 37*, 9877−9883.
(15) Feng, Y. Q., and Sligar, S. G. (1991) Effect of heme binding on the structure and stability of *Escherichia coli* apocytochrome b562. *Biochemistry 30*, 10150−10155.
(16) Cordova, J. M., Noack, P. L., Hilcove, S. A., Lear, J. D., and Ghirlanda, G. (2007) Design of a functional membrane protein by engineering a heme-binding site in glycophorin A. *J. Am. Chem. Soc. 129*, 512−518.
(17) Shinde, S., Cordova, J. M., Woodrum, B. W., and Ghirlanda, G. (2012) Modulation of function in a minimalist heme-binding membrane protein. *J. Biol. Inorg. Chem. 17*, 557−564.
(18) Hubbell, W. L., Cafiso, D. S., and Altenbach, C. (2000) Identifying conformational changes with site-directed spin labeling. *Nat. Struct. Biol. 7*, 735−739.
(19) Steinhoff, H. J. (2004) Inter- and intra-molecular distances determined by EPR spectroscopy and site-directed spin labeling reveal protein-protein and protein-oligonucleotide interaction. *Biol. Chem. 385*, 913−920.
(20) Jeschke, G., and Polyhach, Y. (2007) Distance measurements on spin-labelled biomacromolecules by pulsed electron paramagnetic resonance. *Phys. Chem. Chem. Phys. 9*, 1895−1910.
(21) Dockter, C., Volkov, A., Bauer, C., Polyhach, Y., Joly-Lopez, Z., Jeschke, G., and Paulsen, H. (2009) Refolding of the integral membrane protein light-harvesting complex II monitored by pulse EPR. *Proc. Natl. Acad. Sci. U.S.A. 106*, 18485−18490.
(22) Nicklisch, S. C., Wunnicke, D., Borovykh, I. V., Morbach, S., Klare, J. P., Steinhoff, H. J., and Kramer, R. (2012) Conformational changes of the betaine transporter BetP from *Corynebacterium glutamicum* studied by pulse EPR spectroscopy. *Biochim. Biophys. Acta 1818*, 359−366.
(23) Pfeiffer, M., Rink, T., Gerwert, K., Oesterhelt, D., and Steinhoff, H. J. (1999) Site-directed spin-labeling reveals the orientation of the amino acid side-chains in the E-F loop of bacteriorhodopsin. *J. Mol. Biol. 287*, 163−171.
(24) Perozo, E., Cortes, D. M., and Cuello, L. G. (1998) Three-dimensional architecture and gating mechanism of a K^+ channel studied by EPR spectroscopy. *Nat. Struct. Biol. 5*, 459−469.
(25) Hilger, D., Jung, H., Padan, E., Wegener, C., Vogel, K. P., Steinhoff, H. J., and Jeschke, G. (2005) Assessing oligomerization of membrane proteins by four-pulse DEER: pH-dependent dimerization of NhaA Na^+/H^+ antiporter of *E. coli*. *Biophys. J. 89*, 1328−1338.
(26) Persson, M., Harbridge, J. R., Hammarstrom, P., Mitri, R., Martensson, L. G., Carlsson, U., Eaton, G. R., and Eaton, S. S. (2001) Comparison of electron paramagnetic resonance methods to determine distances between spin labels on human carbonic anhydrase II. *Biophys. J. 80*, 2886−2897.
(27) Banham, J. E., Baker, C. M., Ceola, S., Day, I. J., Grant, G. H., Groenen, E. J., Rodgers, C. T., Jeschke, G., and Timmel, C. R. (2008) Distance measurements in the borderline region of applicability of CW EPR and DEER: A model study on a homologous series of spin-labelled peptides. *J. Magn. Reson. 191*, 202−218.
(28) Haimann, M. M., Akdogan, Y., Philipp, R., Varadarajan, R., Hinderberger, D., and Trommer, W. E. (2011) Conformational changes of the chaperone SecB upon binding to a model substrate—bovine pancreatic trypsin inhibitor (BPTI). *Biol. Chem. 392*, 849−858.
(29) Molin, Y. M., Salikhov, K. M., and Zamaraev, K. I. (1980) *Spin Exchange: Principles and Applications in Chemistry and Biology*, Springer, Berlin.
(30) Parmon, V., Kokorin, A., and Zhidomirov, G. (1977) Conformational structure of nitroxide biradicals use of biradicals as spin probes. In *Journal of Structural Chemistry*, Vol. *18*, pp 104−147, Springer, New York.
(31) Pannier, M., Veit, S., Godt, A., Jeschke, G., and Spiess, H. W. (2000) Dead-time free measurement of dipole-dipole interactions between electron spins. *J. Magn. Reson. 142*, 331−340.
(32) Jeschke, G., Pannier, M., and Spiess, H. W. (2002) Double Electron-Electron Resonance. In *Biological Magnetic Resonance: Distance Measurements in Biological Systems by EPR* (Berliner, L. J., Eaton, S. S., and Eaton, G. R., Eds.) Vol. *19*, Chapter 11, Kluwer, New York.
(33) Stoll, S., and Schweiger, A. (2006) EasySpin, a comprehensive software package for spectral simulation and analysis in EPR. *J. Magn. Reson. 178*, 42−55.
(34) Marzola, P., Pinzino, C., and Veracini, C. A. (1991) Spin-labeling study of human serum albumin in reverse micelles. *Langmuir 7*, 238−242.
(35) Jeschke, G., Bender, A., Paulsen, H., Zimmermann, H., and Godt, A. (2004) Sensitivity enhancement in pulse EPR distance measurements. *J. Magn. Reson. 169*, 1−12.
(36) Jeschke, G., Chechik, V., Ionita, P., Godt, A., Zimmermann, H., Banham, J., Timmel, C., Hilger, D., and Jung, H. (2006) DeerAnalysis2006: A comprehensive software package for analyzing pulsed ELDOR data. In *Applied Magnetic Resonance*, Vol. *30*, pp 473−498, Springer, Weinheim, Germany.
(37) Guskov, A., Kern, J., Gabdulkhakov, A., Broser, M., Zouni, A., and Saenger, W. (2009) Cyanobacterial photosystem II at 2.9-Å resolution and the role of quinones, lipids, channels and chloride. *Nat. Struct. Mol. Biol. 16*, 334−342.
(38) Parmon, V. N., Kokorin, A. I., Zhidomirov, G. M., and Zamaraev, K. I. (1975) On the mechanism of spin exchange in long-chain nitroxide biradicals. *Mol. Phys. 30*, 695−701.
(39) Slichter, C. P. (1955) Spin Resonance of Impurity Atoms in Silicon. *Phys. Rev. 99*, 479−480.
(40) Luckhurst, G. R. (1966) Alternating linewidths. A novel relaxation process in the electron resonance of biradicals. *Mol. Phys. 10*, 543−550.
(41) Glazachev, Y., Khramtsov, V., Berezina, T., and Volodarsky, L. (1998) Imidazoline biradical spin labels with EPR spectral sensitivity to the local concentration of protons. In *Applied Magnetic Resonance*, Vol. *15*, pp 407−415, Springer, Weinheim, Germany.
(42) Parmon, V. N., Kokorin, A. I., Zhidomirov, G. M., and Zamaraev, K. I. (1973) Evidence for slow exchange in E.S.R. spectra of nitroxide biradicals. *Mol. Phys. 26*, 1565−1569.
(43) Hinderberger, D., Jeschke, G., and Spiess, H.-W. (2004) Network formation involving polyelectrolytes in solution: The role of counterions. In *Colloid & Polymer Science*, Vol. *282*, pp 901−909, Springer, Berlin.
(44) Horn, R., Grundmann, G., and Paulsen, H. (2007) Consecutive Binding of Chlorophylls a and b During the Assembly in Vitro of Light-harvesting Chlorophyll-a/b Protein (LHCIIb). *J. Mol. Biol. 366*, 1045−1054.
(45) Horn, R., and Paulsen, H. (2002) Folding in vitro of light-harvesting chlorophyll a/b protein is coupled with pigment binding. *J. Mol. Biol. 318*, 547−556.
(46) Horn, R., and Paulsen, H. (2004) Early steps in the assembly of light-harvesting chlorophyll a/b complex: Time-resolved fluorescence measurements. *J. Biol. Chem. 279*, 44400−44406.
(47) Booth, P. J., and Paulsen, H. (1996) Assembly of light-harvesting chlorophyll a/b complex in vitro. Time-resolved fluorescence measurements. *Biochemistry 35*, 5103−5108.
(48) Booth, P. J., Flitsch, S. L., Stern, L. J., Greenhalgh, D. A., Kim, P. S., and Khorana, H. G. (1995) Intermediates in the folding of the membrane protein bacteriorhodopsin. *Nat. Struct. Biol. 2*, 139−143.
(49) Booth, P. J., Farooq, A., and Flitsch, S. L. (1996) Retinal binding during folding and assembly of the membrane protein bacteriorhodopsin. *Biochemistry 35*, 5902−5909.

(50) Booth, P. J. (1997) Folding α-helical membrane proteins: Kinetic studies on bacteriorhodopsin. *Folding Des. 2*, R85−R92.
(51) Booth, P. J. (2000) Unravelling the folding of bacteriorhodopsin. *Biochim. Biophys. Acta 1460*, 4−14.
(52) Lu, H., and Booth, P. J. (2000) The final stages of folding of the membrane protein bacteriorhodopsin occur by kinetically indistinguishable parallel folding paths that are mediated by pH. *J. Mol. Biol. 299*, 233−243.
(53) Curnow, P., and Booth, P. J. (2010) The Contribution of a Covalently Bound Cofactor to the Folding and Thermodynamic Stability of an Integral Membrane Protein. *J. Mol. Biol. 403*, 630−642.
(54) Tulumello, D. V., and Deber, C. M. (2009) SDS Micelles as a Membrane-Mimetic Environment for Transmembrane Segments. *Biochemistry 48*, 12096−12103.